16th World Conference on Earthquake Engineering, 16WCEE 2017

Santiago Chile, January 9th to 13th 2017

Paper N° 4975 (Abstract ID)

Registration Code: S-U1464633775

MOMENT CONNECTION USING WIDE FLANGE BEAM AND HOLLOW STRUCTURAL SECTION COLUMN IN STEEL MOMENT FRAMES STRUCTURES UNDER SEISMIC LOADS

Eduardo Nuñez C.[1], Ronald Torres[1].

[1]Materials and Structural Models Institute, Faculty of Engineering, Universidad Central de Venezuela, Caracas, Venezuela.

Email: eduardo.imme@gmail.com, ronald.imme@gmail.com

Abstract

The use of Hollow Structural Sections (HSS) provide an alternative for steel buildings in seismic zones, increasing the structural redundancy without incorporating bracings and the performance of flexural, compression and torsion unlike other columns sections. The HSS columns have shown satisfactory performance under seismic loads, as observed in buildings with steel moment frames in the Honshu earthquake (2011). The purpose of this research is to propose a new moment connection, EP-HSS ("End-plate to Hollow Structural Section"), using a wide flange beam and HSS column through a configuration that is out of the range of prequalification established in the ANSI/AISC 358-10 Specification, as an alternative to the traditional configuration of steel moment frames established in current codes. From an analytical, numerical (FEM) and experimental study, based on qualification protocols established in the ANSI/AISC 341-10 Specification, the results showed that the EP-HSS allows the development of inelastic action only on the beam, avoids stress concentration in the column and develops a high energy dissipation capacity, ensuring satisfactory performance under seismic actions without brittle failure mechanisms, satisfying the requirements and protocols established in the AISC (American Institute of Steel Construction) Specifications for seismic zones.

Keywords: *ductility, performance, bolted connection, end-plate connection, hollow structural sections, moment connections, finite element method, steel structure, yield line, seismic design.*

1. Introduction

It is known that the Northridge (1994) and Kobe (1995) earthquakes showed deficiencies in the seismic performance of steel buildings, mainly in the behavior of their connections, initiating a search for new alternatives in configurations of steel structural systems and connections with capacity to achieve an acceptable level of performance. It was observed a big amount of damage in beam-to-column connections in more than 500 buildings, which experienced local buckling in column flanges and webs, bolts fracture, weld fracture, stress concentration in weld zones, due to deficient in welding inspection, inadequate weld design, insufficient width–to-thickness ratios and higher expected strength than nominal strength on materials, showing that the concept of ductile behavior of steel moment frames was incomplete. In particular, the Council of Applied Technology, University Consortium and the Society of Civil Engineers of California, presented proposals in the FEMA 350 [11] after numerous studies, where more than 30 connections were proposed as an alternative to the previously designed, showing better behavior referred to stiffness and strength. Posteriorly, it was introduced the ANSI/AISC 358-10 [2], with 8 connections for use in seismic design of steel moment frames, where only one connection is permitted using HSS columns. Additionally, the columns are contemplated as concrete filled column and the beams are connected to the column with patented brackets. However, the Honshu (2011) earthquake showed that steel moment frames with HSS columns had satisfactory performance under seismic loads. Currently, the research on seismic moment connections in steel moment frames has mainly focused on welded connections between WF beam to HSS column, HSS beam to HSS column, and WF beam to WF column (welded and bolted for this type). Some these investigations are described below.

Regarding the use of the HSS in moment connections, Fadden M. [10] studied the cyclical behavior of HSS to HSS moment connections under seismic loads and proposed welded connections that enhance the performance of welded connections, ensuring the energy dissipation in the beam by incorporating plates in the connection. It was not contemplated the use of a bolted connection, being necessary to perform field welding. Similarly, Gholami M. [13] studied the behavior of welded connections between WF beam to Box Section column, finding an adequate performance with the addition of plates in beam flanges and web, where the field welding will also be necessary for the use of this connections. Recently, Chao Yang [7] conducted an investigation where he behavior of the "ConXL" connection was characterized from models using finite elements, with concrete filling and without concrete filling in the column. The results showed that this configuration can meet ductile failure mechanism as contemplated in the ANSI/AISC 358-10 [3],. Additionally, various "ConXL" connection joint configurations without concrete filling in the column showed beam hinge mechanism failure mode when the axial load level in the column is not too high (~0.4). However, the failure mode becomes beam–column hinge hybrid failure mechanism or even column hinge mechanism with an increase in the axial load level. Finally, the connection is proposed with patented brackets. Likewise, Blaž Čermelj [4][5] conducted a study using numerical methods from prior testing, between WF beam to Box Section column with welded plates that reinforce the connection. Additionally, they studied the influence of complete joint penetration welds, achieving acceptable performance in those connections that use CJP, where field welding is necessary for the use of this connections.

Therefore, it is necessary to develop a beam-to-column connection using WF beam to HSS column in steel moment frames for building structures under seismic loads, through the qualification of a bolted moment connection, using a design procedure from an analytical, numerical (FEM) and experimental study based in the requirements and protocols established in the AISC Specifications [1][2], for seismic zones, with the goal of avoiding the use of field welding.

2. Description of EP-HSS Moment Connection

The EP-HSS (End-Plate to Hollow Structural Section) is a new alternative for moment connections in Steel Moment Frame Buildings, where wide flange beams are connected to HSS columns. The configuration has end-plates connected by high strength bolts, which are connected with external diaphragms to the HSS column for transferring the flexural strength from the beam. A combination of fillet and complete joint penetration welds was used between plates to column and end-plates, respectively. Furthermore, this configuration allows a simple erection in field due to the beams that are completely bolted in site, avoiding field welding and minimizing complications associated with their assembly and inspection in site.

In this investigation, an internal node configuration from a 4-story residential building in seismic zone was obtained. The design was made from compliance of the requirements of the AISC Specifications [1][2], the column plates design is highly controlled by the maximum expected flexural strength of beam. Likewise, bolts and the end-plate thickness are designed with the maximum expected flexural strength of the beam, according to ANSI/AISC-358-10 Specification [2]. Once the process design was completed, an IPE-200 beam was obtained (with dimensional properties: thickness flange tf = 8.5 mm, thickness web tw = 5.6 mm, d = 200 mm and bf = 100 mm), an ECO-220x220x9 column (HSS with dimensional properties: b= 220 mm, h = 220 mm, tf = 9 mm), eight ASTM-A-325 3/4" bolts, two end-plates (tp=22 mm for each plate), two horizontal reinforcement plates in column (tp=16 mm), a vertical reinforcement plate in column (tp=8 mm) and E70XX electrodes for the welding, as shown in Figure 1.

Table 1. Material parameters of steel members.

Member	Designation	Yield Strength (MPa)	Ultimate Strength (MPa)
Column: HSS 220x220x9	ASTM-A-500 Gr. B	351	408
Beam: IPE-200	ASTM-A-36	253	408
End-plate	ASTM-A-36	253	408
Plate	ASTM-A-36	253	408
High Strength Bolt	ASTM-A-325	632	843

[Note]: Young's modulus of all metals E = 210,000 MPa, Poisson's ratio ν = 0.3. All properties shown in the table are nominals.

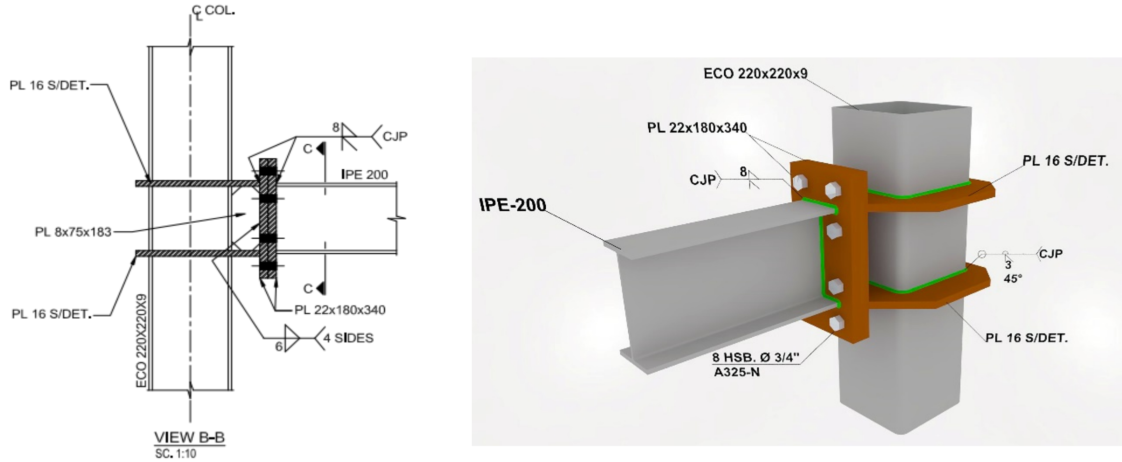

Figure 1. Details of EP-HSS Moment Connection.

3. Analytical Model of EP-HSS Moment Connection

In this investigation, the beam depth is out of the prequalification range, but this concept is extrapolated as hypothesis due to the similarity of the connection with the established in the ANSI/AISC-358-10 Specification [2]. Where *bp* is the width of the plate, *g-s- pfo - Pfi- de- ho- hi* are distances as shown in Figure 2, F_y is the Yield Strength of the end-plate and M_f the moment at column face. As show in figure (2), the end-plate strength is obtained from nine yield lines, of which only eight yield lines (from yield line 2 to yield line 9) allows to obtain the same *"Yp"* parameter proposed by the AISC-358-10 Specification [2], obtaining the *"tp"* thickness of the plate. However, if the resistance of the plate is estimated from the all yield lines (from yield line 1 to yield line 9), is obtained another "$Yp_{EP\text{-}HSS}$" parameter, which allows to obtain a smaller thickness plate, due to the additional strength provided by the yield line 1, with similar performance for seismic design.

3.1 Yield Lines of the EP-HSS

First, it will be taken the yield lines from 2 to 9, without the yield line 1 to obtain the *"Yp"* parameter of the Specification [2], being necessary to calculate the virtual displacements and rotations in the connection, as shown in the equations 1, 2, 3 and table (2).

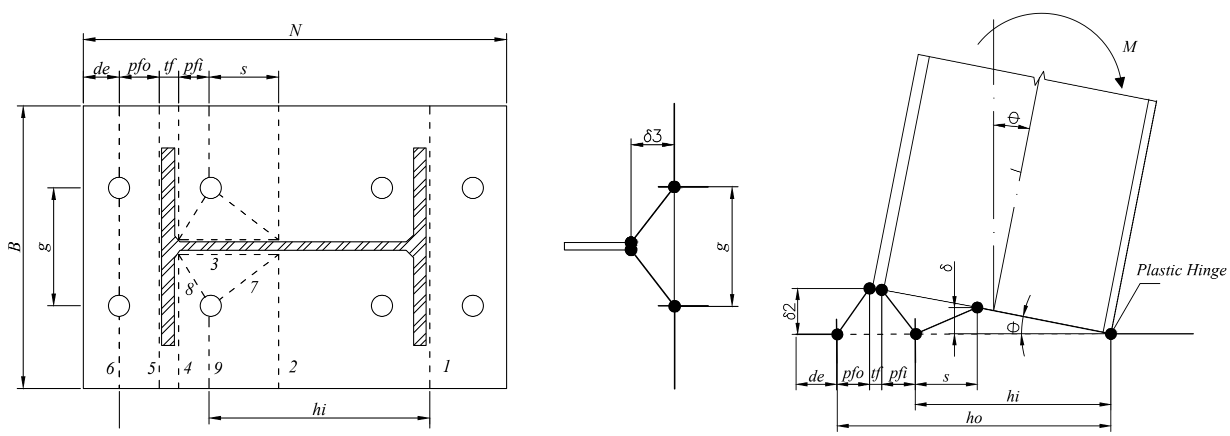

Figure 2. Yield line pattern for EP-HSS Moment Connection.

The Virtual displacements *(δ_i)* in the connection was obtained as follow:

$\delta = \theta(d/2)$ $\quad Eq.(1)$ $\qquad \delta_2 = \theta(h_o - p_{fo})$ $\quad Eq.(2)$ $\qquad \delta_3 = \theta h_i$ $\quad Eq.(3)$

The same procedure, with the difference, includes the additional strength provided by the yield line 1 shown in Figure (2), an alternative *"$Yp_{EP\text{-}HSS}$"* parameter is obtained, which optimizes the thickness of the end-plate. In the table (2) are shown the virtual displacements and rotations in the connection, including all the yield lines.

Table 2. Virtual rotations (θ) and yield lines length (l):

Yield line	*Length (li)*	*Rotation (θi)*
1	B	θ
2	$B/2$	$\theta(h_i/s-1)+\theta$
3	$p_{fi}+s$	$2\theta(h_i/g)$
4	$B/2$	$\theta\left(\frac{h_i}{p_{fi}}+1\right)-\theta$
5	B	$\theta\left(\frac{h_o}{p_{fo}}-1\right)+\theta$
6	B	$\theta\left(\frac{h_o}{p_{fo}}-1\right)$
7	L_7	$\frac{\theta h_i}{L_7}\left(\frac{g}{2s}+\frac{2s}{g}\right)$
8	L_8	$\frac{\theta h_i}{L_8}\left(\frac{g}{2p_{fi}}+\frac{2p_{fi}}{g}\right)$
9	$B-{}^{g}/_{2}$	$\theta\left(\frac{h_i}{p_{fi}}+\frac{h_i}{s}\right)$

$$Y_{pEP-HSS}=\left\{b_p/2\left[h_i\left(\frac{1}{s}+\frac{1}{p_{fi}}\right)+\left(\frac{h_o}{p_{fo}}\right)\right]+\frac{2}{g}h_i\left(p_{fi}+s\right)\right\} \qquad \textit{Eq. (4)}$$

The equation 4 shows a new *"$Yp_{EP\text{-}HSS}$"* parameter, which reduces the thickness of the end-plate from 22mm to 19mm. The numerical study of both proposals are shown in section 4.

4. Numerical model of EP-HSS Moment Connection

A numerical analysis of two models of connections using the Finite Element Method (FEM) with ANSYS v14 [3] was performed. The first model analyzed, EP-HSS (1), is obtained from the design of the connection with the pattern of yield lines established in ANSI/AISC-358-10 Specification [2] and the second model analyzed, EP-HSS (2), is obtained with the same procedure according to Specification, but using the *"$Yp_{EP\text{-}HSS}$"* parameter proposed in the section 3 based in *Eq. (4)*. The numerical study was performed employing the nonlinear characteristics of the material, geometrics nonlinearities and contact nonlinearities or boundary conditions. The large deflections effects were considered in the simulations due to high rotations level reached in the connections, according to Diaz, C. [8][9].

4.1 Element type and mesh

The SOLID elements have their defined geometry through its nodes and can be used to idealize structural elements of any geometry, especially volumetric structures, where the three main dimensions are similar or where it is necessary to consider the deformation of an element in all directions. Therefore, the model was built using hexahedral and tetrahedral 3D solid elements (SOLID 186) in stiffeners, plates, bolts, beams, column and nuts, avoiding conflicts may arise occasionally in the interaction between elements of different types (PLANE, SHELL). The SOLID186 elements allowed the formulation of materials with plasticity, hardness, yield strength, large deflections and large deformations. This element has three translational degrees of freedom per node and comprises 20 nodes [3]. In order to obtain a better computational efficiency and fast convergence, a refined mesh in areas where large inelastic incursions are expected and gross mesh in other areas was performed. The mesh refinement can be shown in the figure (3), where the difference observed between the meshing done. The number of elements and nodes of the end-plate, column and beam shown in table (3), being the same for both models.

Table 3. Number of elements and nodes in FEM models.

Model	End-plate		Column		Beam	
	Number of elements	Number of nodes	Number of elements	Number of nodes	Number of elements	Number of nodes
EP-HSS (1)	3147	17380	9152	61992	2583	18222
EP-HSS (2)	3147	17380	9152	61992	2583	18222

[Note]: EP-HSS (1), model with *"Yp"* Parameter. EP-HSS (2), model with *"$Yp_{EP\text{-}HSS}$"* parameter.

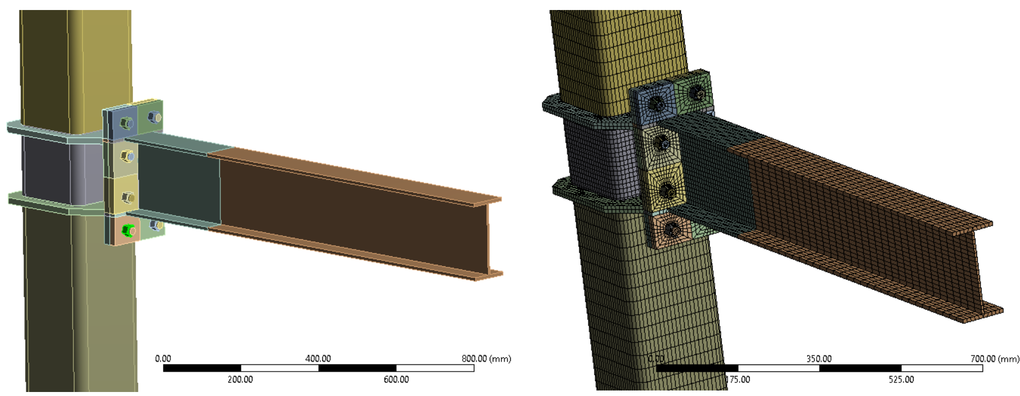

Figure (3). Mesh of EP-HSS moment connection.

4.2 Boundary conditions, contacts and loading

In each finite element model were assigned constraints at the ends of the column, being the displacements fixed and pinned the rotations for to simulate the conditions of the experimental study and in the beam, the displacement is located in free end joint. The displacement was applied according to the protocol established in the ANSI/AISC 358-10 Specification [2] in the free end joint. The restrictions were assigned with the "Remote Point Displacement" command in beam and column of each model. Likewise, the bolt pretension was assigned, according to 70% of the nominal tension strength. These conditions are showed in Figure (4) and the load sequence of test and FEM in table (4). The contact between end-plates is type "Frictional", which allows the separation between the connected elements and takes the friction of tangential movement between these elements. The friction coefficient was assumed μ = 0.3, according to Diaz, C. [8][9]. The contact between bolts and nuts were simulated using contacts type "Frictionless" which allows separation between the connected parts and allows the tangential movement without considering the friction, according to research conducted by Soo Kim [17]. The connection between the column-rings, iron extreme-beam, iron extreme-rings, iron extreme-stiffener, stiffeners-column and stiffeners-rings, was used a contact type "Bonded" which prohibits movement between the parts in contact, such it generates as a welded joint.

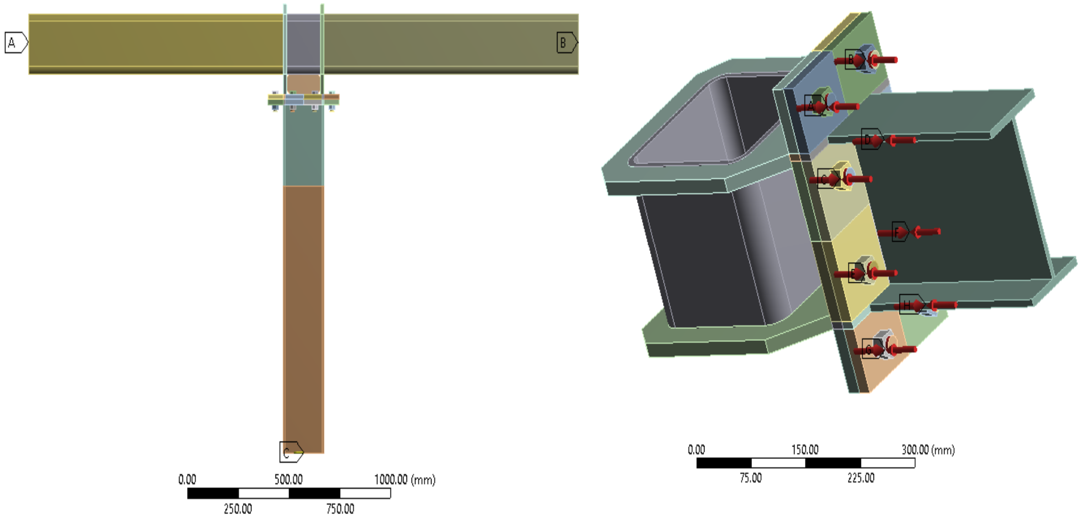

Figure (4). Boundary conditions and bolt pretension assigned. In the left side, is showed in "A" and "B" points the end joint column. The "C" point is the free end joint beam. In the right side, is showed the bolt pretension in the EP-HSS moment connection.

Table 4. Load protocol of test and FEM.

No.	No. of cycles	Drift angle (θ) radians
1	6	0.00375
2	6	0.005
3	6	0.0075
4	4	0.01
5	2	0.015
6	2	0.02
7	2	0.03
8	2	0.04

Note: continue loading at increments of θ=0.01 rad, with two cycles of loading at each step.

4.3 Material modelling

The FEM used different steel types for beams, columns, vertical and horizontal stiffeners, and bolts. The steel stress-strain relationships are defined as multi-linear forms. Currently, a multi-linear kinematic hardening rule with Von-Mises yielding criterion form of stress-strain relationship is commonly used to simulate metal plasticity loading in practical analyses. Additionally, actual material properties from tensile tests were converted and idealized to true stress and true strain values and then input and applied to FEM models, as showed in table (5).

Table 5. Material properties from tensile specimen.

Element	Designation	Yield Stress σ_y (MPa)	Yield Strain ε_y(mm/mm)	Ultimate Stress σ_u (MPa)	Ultimate Strain ε_u(mm/mm)
Beam, Stiffeners, End-plates	ASTM-A-36	380	0.0018	575	0.20
Column	ASTM-A-500 Gr. B	496	0.0025	597	0.01
Bolt	ASTM-A-325	634	0.0036	848	0.14

4.4 Results of EP-HSS (1) FEM model

The connection model EP-HSS (1) reached a maximum load of 66.14 KN and flexural strength 1.8 times the nominal flexural strength of the beam and maximum drift reached of 0.05 radians. Also, a good performance in the connection was observed by inelastic incursion of the beam, as shown by the hysteretic cycles where there is no evidence of brittle failure mechanisms, due to the elastic behavior of the elements that make the connection range. In addition, hysteretic cycles exhibit degradation stable stiffness even 0.01 radians where degradation of 2% and a degradation of 54% to 0.04 radians is achieved due to the inelastic incursion of the beam relative to initial stiffness. As shown in Figure (6) and figure (7), a stress concentration in the beam, above the expected yielding values and deformations exceed the elastic limits is obtained. Similarly, the column and the connection elements do not experience incursion inelastic, being exclusively inelastic beam where all action is concentrated.

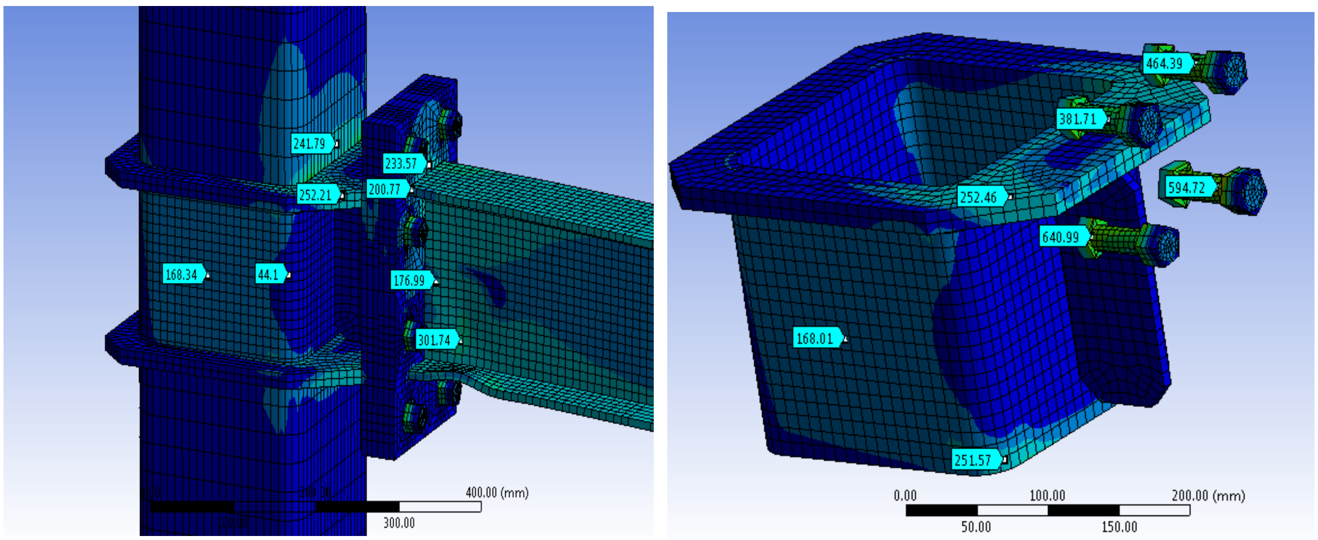

Figure (6). Von-Mises equivalent stress distribution at the maximum load point of EP-HSS (1) in MPa units.

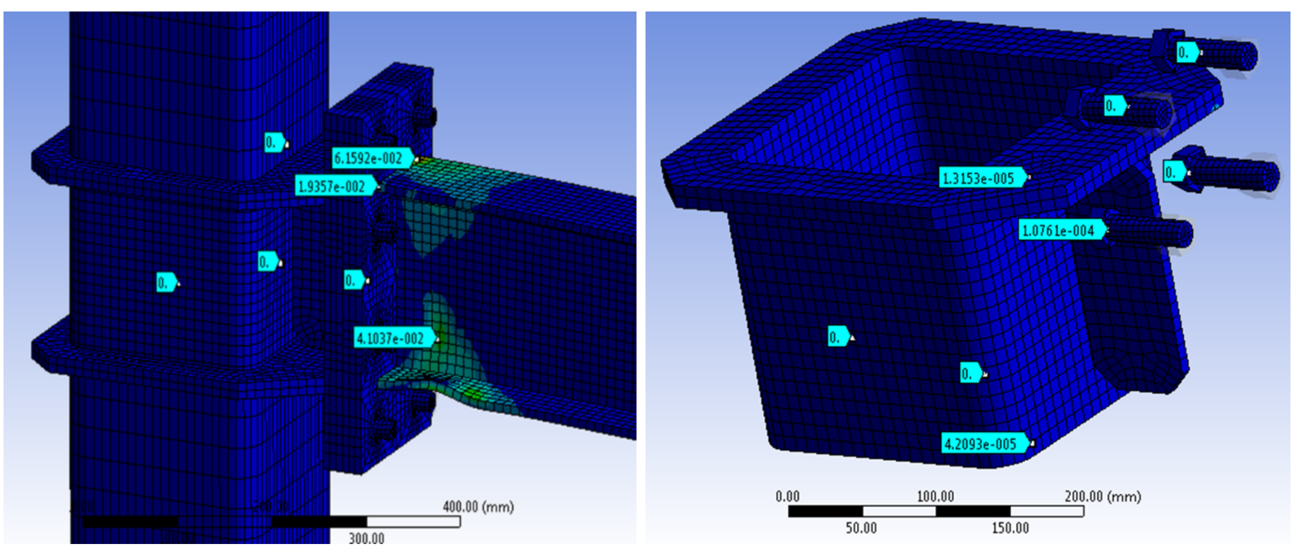

Figure (7). Plastic deformations at the maximum load point of EP-HSS (1) in mm/mm units.

4.5 Results of EP-HSS (2) FEM model

The connection model EP-HSS (2) reached a maximum load of 66.46 KN and flexural strength 1.82 times the nominal flexural strength of the beam and maximum drift reached of 0.05 radians. Also, a good performance in the connection was observed by inelastic incursion of the beam, as shown by the hysteretic cycles where there is no evidence of brittle failure mechanisms, due to the elastic behavior of the elements that make the connection range. In addition, hysteretic cycles exhibit degradation stable stiffness even 0.01 radians where degradation of 16% and a degradation of 56% to 0.04 radians is achieved due to the inelastic incursion of the beam relative to initial stiffness. As shown in Figure (8) and figure (9), it was obtained a stress concentration in the beam above the expected yielding values, and deformations that exceed the elastic limits. Similarly, the column and the connection elements do not experience inelastic incursion, being the beam exclusively inelastic, where all action is concentrated. This behavior is associated with a ductile failure mechanism and therefore it is desired according to seismic design philosophy.

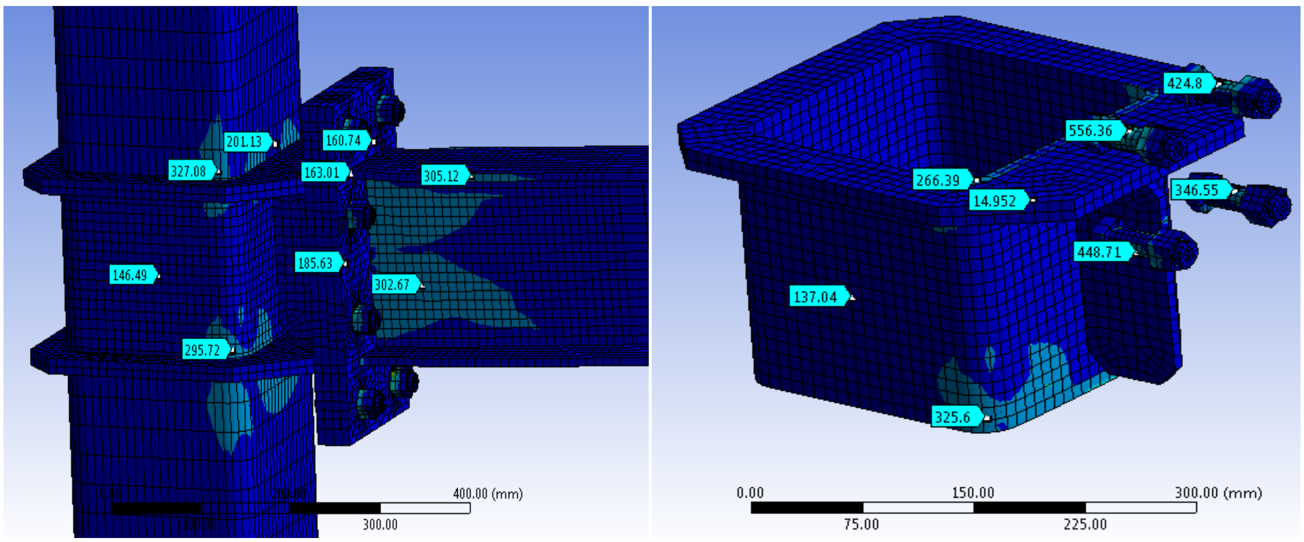

Figure (8). Von-Mises equivalent stress distribution at the maximum load point of EP-HSS (2) in MPa units.

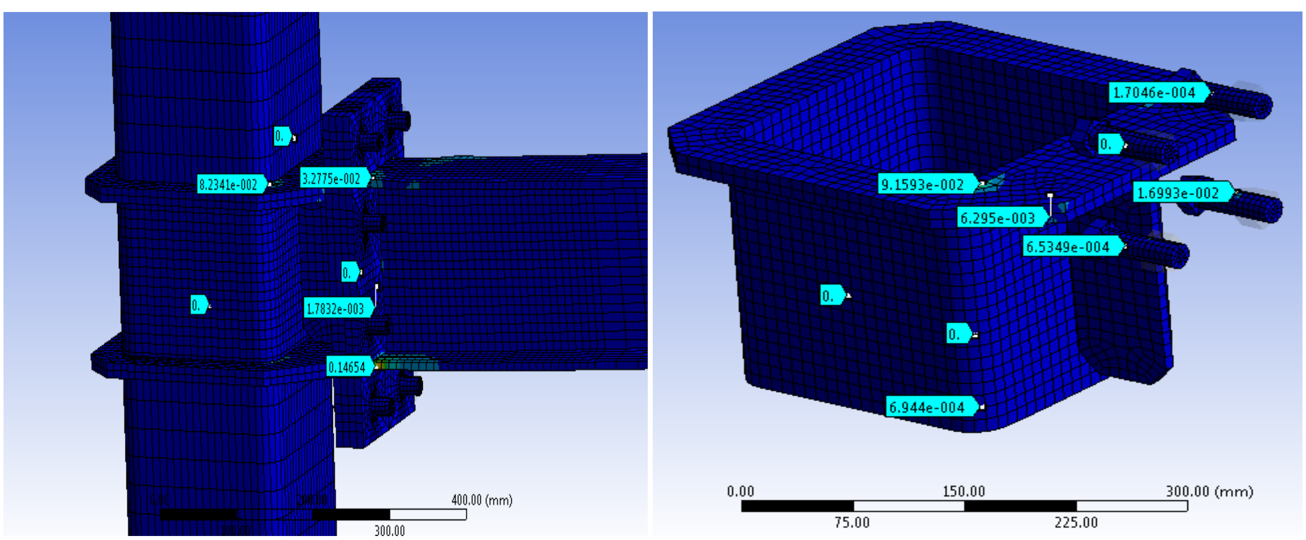

Figure (9). Plastic deformations at the maximum load point of EP-HSS (2) in mm/mm units.

5. Experimental study of EP-HSS Moment Connection

In order to validate the experimental study, three specimens were tested with the same characteristics described for the EP-HSS (1) Moment connection. The EP-HSS (2) was not performed because acceptable calibration between EP-HSS (1) model and the experimental results is obtained. The instrumentation consists of 3 LVDT (linear variable speed power transformer) that capture the desired displacement. The LVDT-1 was located in the actuator positioned in the end of beams and to capture the displacement applied. The LVDT-2 and LVDT-3 at end of columns to verify if there was any movement, as indicated in figure (10). The load capacity is 50 tonf and has a maximum displacement of ±125mm. Actuator specifications are Force

Transducer, model 661.23F -01 SN: 0375349 manufactured by MTS Systems Corporation USA. The displacement applied by the actuator is performed as indicated in figure (10), which describes loading protocol as indicated in ANSI/AISC 341-10 Specification [1], described in the table (4).

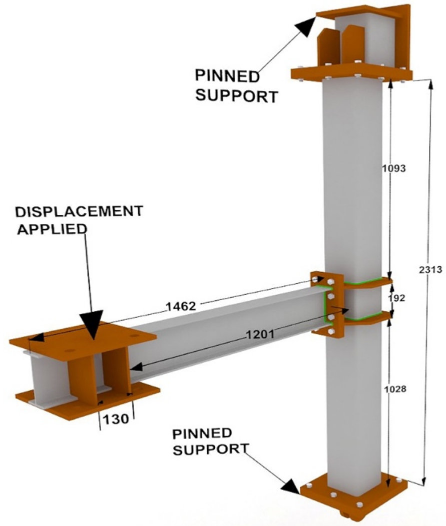

Figure 10. Dimensions and instrumentation of EP-HSS (1) Moment Connection.

The results show the following: the specimen 1, reached a maximum load of 65.26 KN and 1.79 times the nominal flexural resistance of the beam and a maximum drift reached of 0.06 radians. The hysteretic cycles exhibit stiffness stable until a degradation of 0.01 radians where the degradation was of 8%, reaching 65% degradation to 0.04 radians due to inelastic incursion of the beam respect to initial stiffness. The column and connection elements do not experience inelastic incursion, being only the beam where all inelastic action is concentrated, showing a ductile failure without occurrence of brittle failure. Importantly, the specimen # 1 shows an initial disturbance in curves, due to decoupling during the experimental phase, which was solved without major problems for continuity testing and subsequent tests. The specimen 2, reached a maximum load of 71.90 KN and 1.97 times the nominal flexural resistance of the beam and a maximum drift reached of 0.05 radians. The hysteretic cycles exhibits a stable stiffness until a degradation at 0.01 radians where the degradation was of 13%, reaching 64% degradation to 0.04 radians due to inelastic incursion of the beam respect to initial stiffness. The column and connection elements do not experience inelastic incursion, being only the beam where all inelastic action is concentrated, showing a ductile failure without occurrence of brittle failure. The specimen 3, reached a maximum load of 70.70 KN and 1.93 times the nominal flexural resistance of the beam and a maximum drift reached of 0.05 radians. The hysteretic cycles exhibit stable stiffness until a degradation at 0.01 radians where the degradation was of 5%, reaching 60% degradation to 0.04 radians due to inelastic incursion of the beam respect to initial stiffness. The column and connection elements do not experience inelastic incursion, being only the beam where all inelastic action is concentrated, showing a ductile failure without occurrence of brittle failure.in the table (6) are resumed values obtained in the FEM.

Table 6. Summary of maximum values obtained in tests and FEM.

Type of Connection	Max. Load (KN)	Max. Displacement (mm)	Initial Stiffness (KN/mm)	Dissipated Energy (KN-mm)	Max. Moment (KN.mm)	Max. Rotation (rad)
EP-HSS (1)	66.14	76	4979	40532	99.20	0.05
EP-HSS (2)	66.46	76	4844	36171	99.69	0.05
Test 1	65.26	90	6933	58140	97.89	0.06
Test 2	71.90	75	7451	44126	107.85	0.05
Test 3	70.70	75	6519	53543	106.05	0.05

5.1 Results of experimental study and comparisons with FEM.

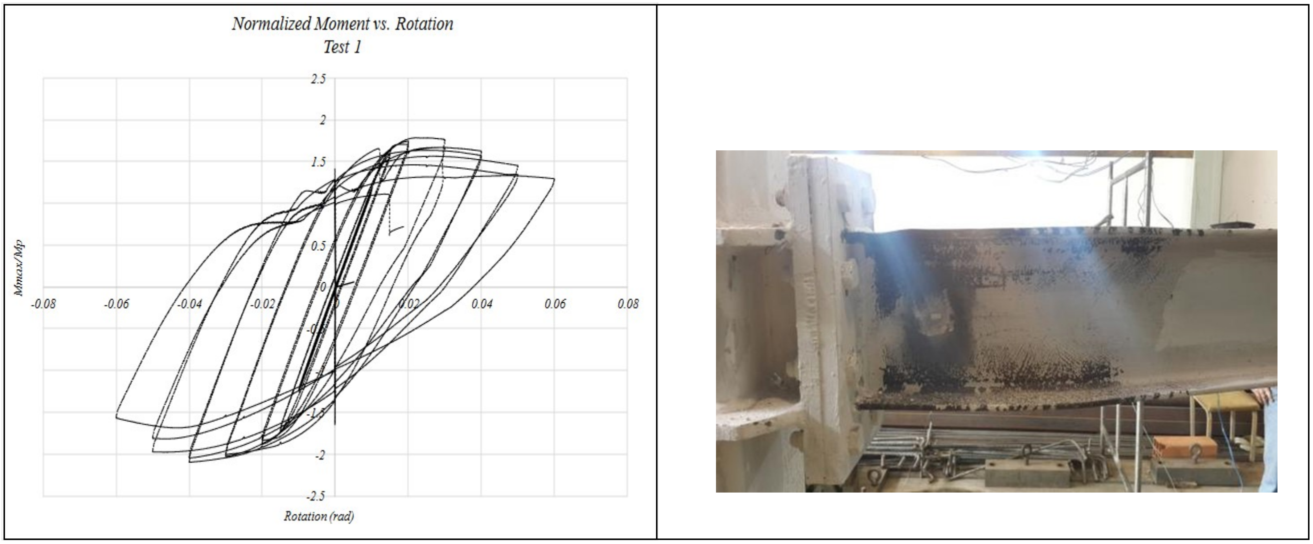

Figure 11. Results of Test 1.

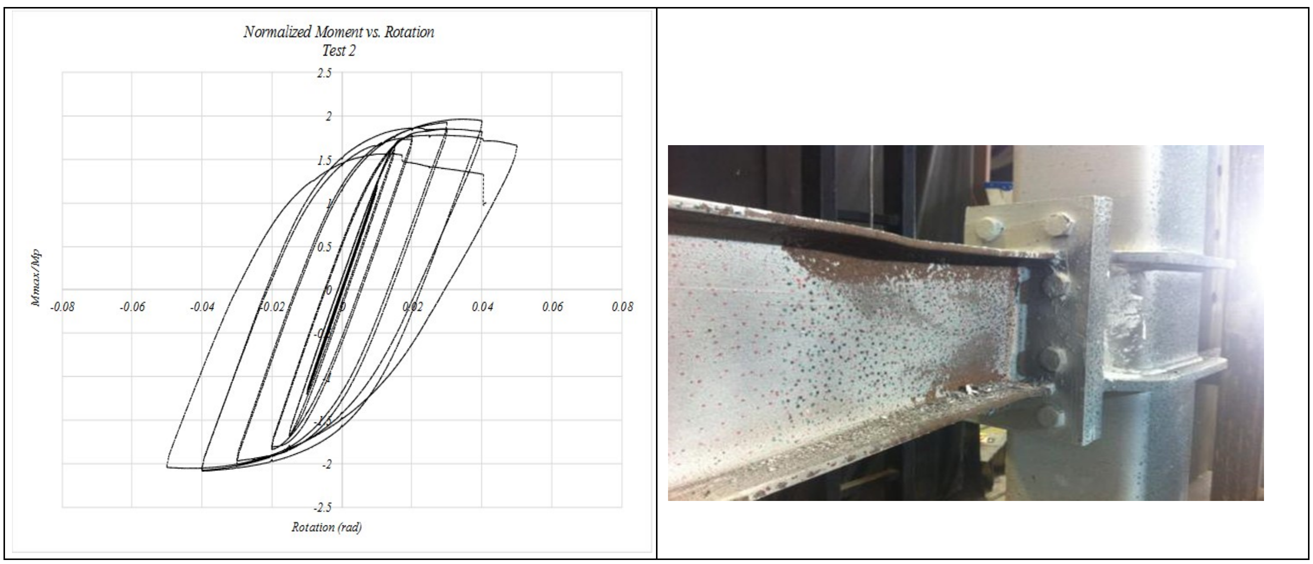

Figure 12. Results of Test 2.

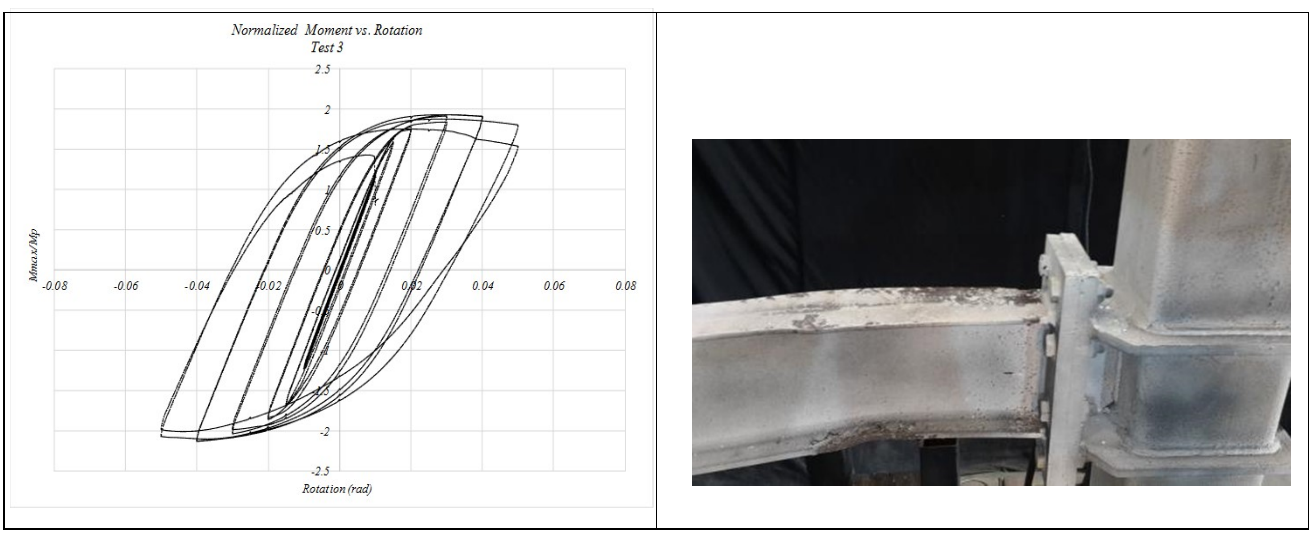

Figure 13. Results of Test 3.

Table 7. Comparison of resistances to bending and expected nominal in tests and FEM.

Type of Connection	M / Mp	M / Mpe	M / 0.8Mp
EP-HSS (1)	1.80	1.21	2.26
EP-HSS (2)	1.82	1.21	2.27
Test 1	1.79	1.19	2.23
Test 2	1.97	1.31	2.46
Test 3	1.93	1.29	2.42

[Note]: M: Moment obtained, Mp: Plastic Moment, Mpe: Expected Plastic Moment.

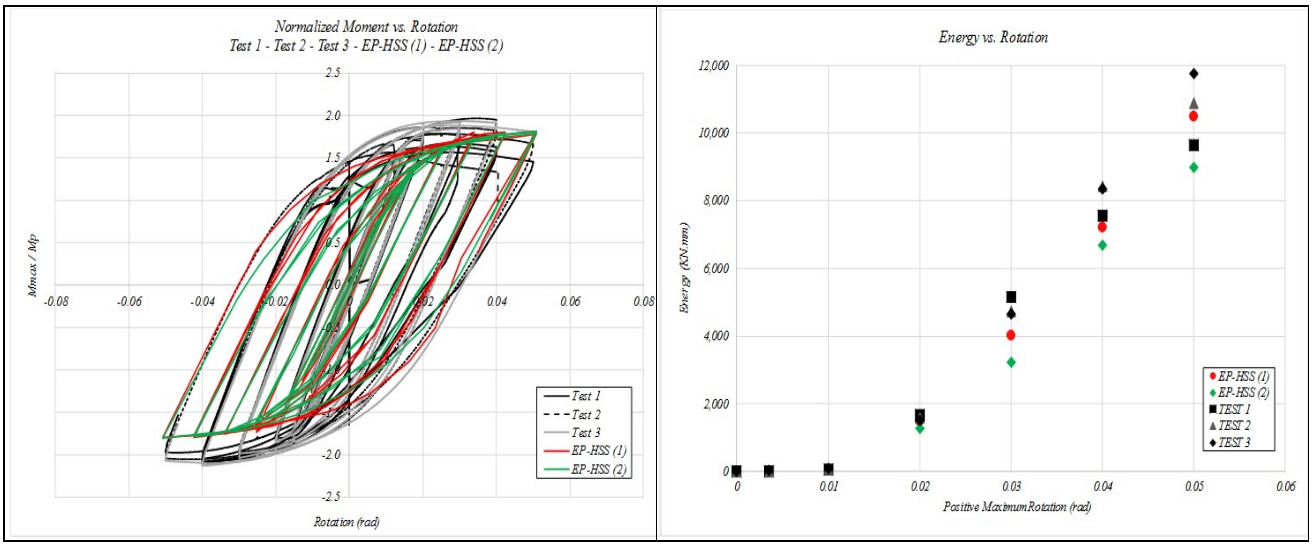

Figure 14. Comparison between Tests and FEM models.

As shown in figures (11), (12) and (13), a repeatability of performance in the tests was obtained, having increased stiffness in the specimen 2 and specimen 3 unlike the specimen 1. Further, the values of flexural resistance are largely superseded on what established protocol qualification according to ANSI/AISC 341-10 [1]. The FEM models show a similar performance even when they have different thicknesses of end-plate, ensuring the performance required by the current seismic design philosophy. As shown in Figure (14), a comparison between experimental specimens and FEM models was performed. A slight difference was also observed in the stiffness, which affects the energy dissipated. In the FEM models, the flexural resistance and maximum rotation obtained models are similar, having an evolution of dissipated energy respect to rotation reached. Similarly, the dissipated energy was obtained, observing that the energy obtained in the tests is greater than the energy dissipated in the MEF models. In particular, the specimen 1 dissipates 1.6 times more that EP-HSS (2) and 1.4 times more that EP-HSS (1). The specimen 2, dissipates 1.2 times more that EP-HSS (2) and 1.1 times more that EP-HSS (1). The specimen 3, dissipates 1.5 times more that EP-HSS (2) and 1.3 times more that EP-HSS (1). In general, the tested specimens dissipate on average 1.36 times more energy than models in FEM, because the specimens tested had a higher capacity for the same level of deformation. Table 7 shows a comparison of the relationship between time points obtained and nominal moments or expected time, showing that both models in FEM and the specimens tested, reached a flexural resistance greater than nominal plastic moment, complying with the conditions of AISC Specifications [1][2].

6. Conclusions.

It was verified analytically fault pattern established in the ANSI/AISC 358-10 [2] for End-plate type connections, noting that it is possible to establish an alternative pattern that allows a thickness reduction of 16%, without evidence of a fragile connection failure. Simulations in FEM of EP-HSS (1) and EP-HSS (2) connections showed a satisfactory performance, reaching a flexural resistance above 1.8 times of the nominal flexural resistance and rotation capacity of 0.05 radians. Failure concentrated on the beam, complying with seismic design philosophy where the beam is the fuse element Special Moment

Frames, allowing inelastic action is out of the connection to the column. Vertical stiffeners and Horizontal stiffeners allowed transmit the flexural resistance of the beam, ensuring stable hysteretic cycles without degradation of rigidity and strength. Full-scale specimens of EP-HSS (1) moment connection were performed obtaining a favorable performance where resistance exceeded 1.9 times the flexural resistance in the beam and exceeded stably 0.04 radians required by that standard. No brittle failure mechanism associated with the local buckling column, plates or stiffeners, and failures of the bolts for all cycles were observed. All inelastic action was presented in the beam, where from 0.05 radians local buckling in flanges and webs was observed. In order to the dissipate energy, increased dissipated energy as rotation cycles are reached in FEM models and tested specimens were observed. In general, the tested specimens dissipate on average 1.36 times more energy than the average energy dissipated in FEM models because simulations achieved convergence until fewer cycles the specimens. Finally, the EP-HSS (1) connection is an alternative for moment connections between I beams and HSS columns, outside of prequalification range established in ANSI/AISC 358-10 [2], allowing its use in Special Moment Frames satisfying with the seismic design philosophy.

7. References.

[1] AISC: ANSI/AISC 341-10. Seismic provisions for structural steel buildings. Chicago, IL: American Institute of Steel Construction; 2010.
[2] AISC: ANSI/AISC 358-10. Prequalified connections for special and intermediate steel moment frames for seismic applications. Chicago, IL: American Institute of Steel Construction; 2010.
[3] ANSYS. ANSYS. Theory reference. Canonsburg, PA: ANSYS Inc.; 2005.
[4] B. Čermelj, D. Beg, Cyclic behaviour of welded stiffened beam-to-column joints — experimental tests, Steel Constr. 7 (2014) 221–229.
[5] Blaž Čermelj, Primož Može, y Franc Sinur. On the prediction of low-cycle fatigue in steel welded beam-to-column joints. Journal of Constructional Steel Research Volume 117, February 2016, Pages 49–63.
[6] Bruneau, M., Uang, C.-M., Sabelli, R. 2011. “Ductile design of steel structures.” McGraw Hill, Boston, MA.
[7] Chao Yang, Jun-Fen Yang, Ming-Zhou Su, Cheng-Zong Liu (2016). Numerical study on seismic behaviors of ConXL biaxial moment connection. Journal of Constructional Steel Research Volume 121, June 2016, Pages 185–201.
[8] Díaz, C. Tesis Doctoral. “Diseño óptimo de uniones semirrígidas mediante simulación numérica y modelos Kriging”. Universidad Politécnica de Cartagena. 2013.
[9] Díaz C., Victoria M., Martí P, Querin OM. FE model of beam-to-column extended end-plate joints. J. Constr. Steel Res. 2011;67:1578–90.
[10] Fadden M. Cyclic Bending Behavior of Hollow Structural Sections and Their Applica- tion in Seismic Moment Frame Systems. (Dissertation) Ann Arbor: University of Michigan; 2013.
[11] Federal Emergency Management Agency (FEMA). Recommended seismic design criteria for new steel moment-frame buildings (FEMA-350). Washington, D.C.; 2000.
[12] Ghassemieh, M. Evaluation of Stiffened End-Plate Moment Connection through Optimized Artificial Neural Network. School of Civil Engineering, University of Tehran, Tehran, Iran. Journal of Software Engineering and Applications, 2012, 5, 156-167.
[13] Gholami M., Deylami A., Tehranizadeh M. Seismic performance of flange plate connections between steel beams and box columns. Journal of Constructional Steel Research Volume 84, May 2013, Pages 36–48.
[14] Herrera RA, Bravo M, GómezG, Aedo G. Performance of built-up T-stubs for Double T moment connections. J. Constr. Steel Res. 2013, 88:289–95.
[15] L.H.Han, W.D. Wang, X.L.Zhao, Behaviour of steel beam to concrete filled SHS column frames: finite element model and verifications, Eng. Struct. 30 (2008) 1647–1658.
[16] M. Wang, Y.J. Shi, Y.Q. Wang, et al., Numerical study on seismic behaviors of steel frame end-plate connections, J. Constr. Steel Res. 90 (2013) 140–150.
[17] Soo Kim, T., & Kuwamura, H. 2007. Finite element modeling of bolted connections in thin-walled stainless steel plates under static shear. Thin-Walled Structures, 45(4), 407– 421.